

Above-Threshold Ionization with Elliptically Polarized Light

M. Bashkansky,^(a) P. H. Bucksbaum, and D. W. Schumacher

AT&T Bell Laboratories, Murray Hill, New Jersey 07974

(Received 1 May 1987)

Above-threshold multiphoton ionization angular distributions have been studied for elliptical laser polarization in xenon and krypton. In contrast to previous linear and circular polarization studies, the angular distributions are strongly dependent on the order of the above-threshold-ionization peak, even for very high-energy electrons. This provides a new test for theories of atomic photoionization in intense laser fields. A standard nonperturbative model, when generalized to accommodate elliptical polarization, is found to yield angular distributions which are in reasonable accord with experimental results.

PACS numbers: 32.80.Rm, 42.50.Hz

Multiphoton ionization of atoms at high intensities, where the electron's classical "wobble" energy approaches the atomic binding energy, has attracted widespread recent attention. The theoretical problem, in which the radiation field cannot be represented as a small perturbation of the atomic Hamiltonian, has yet to be solved, but many approximations have been studied.¹⁻⁸ As a result of the rapid advance in the technology of high-powered lasers, experiments may now be performed at wavelengths from 250 nm to 10 μm .

Photoelectron angular distributions are an important tool for comparing models to experiments. Previous angular distribution measurements in xenon and other rare gases, utilizing linearly polarized neodymium-doped yttrium aluminum garnet radiation ($\lambda = 1.06 \mu\text{m}$), have revealed the presence of ponderomotive scattering as a result of the large intensity gradients in the laser focus.⁹ Furthermore, when the ponderomotive forces are less significant, namely, for lower intensity, shorter wavelength or higher electron final energy, experiments show that electrons are mostly emitted in the direction of the classical driving force along the laser polarization $\hat{\epsilon}$.¹⁰ Of course, for circular polarization, the distributions must be azimuthally isotropic.

The current work extends the study of angular distributions of above-threshold multiphoton ionization (ATI) electrons to elliptical polarization. In contrast to linear or circular polarization, the angular distributions are found to be strongly dependent on the order of the ATI peak. The distributions are also strong functions of the polarization retardation, particularly when the polarization is nearly circular. These new phenomena may be valuable tests of ATI theories. At present, few predictions exist for elliptically polarized ATI; however, we find that a straightforward extension of nonperturbative theories¹ that treat the laser field classically, are in striking agreement with these angular dependences.

The experiments were performed using 1064-nm 100-ps pulses from an amplified neodymium-doped yttrium aluminum garnet laser, focused into an ultrahigh-vacuum chamber containing a low density (10^{-10}

cm^{-3}) of xenon or krypton. The focal waist was approximately 10 μm and peak intensities ranged as high as $2.4 \times 10^{14} \text{ W/cm}^2$. Electron energies were analyzed by time of flight. The apparatus has been described in detail elsewhere.¹¹ The desired polarization was obtained by means of half-wave and quarter-wave retardation plates inserted into the laser beam. By rotating the two plates with respect to each other, any desired retardation and orientation could be achieved. The polarization state was monitored directly with a rotating linear polarizer.

Figure 1 shows a typical series of retardation spectra for xenon, obtained at a laser intensity of $5.0 \times 10^{13} \text{ W/cm}^2$. The retardation angle is ξ , where the polarization is given by $\hat{\epsilon} = \hat{x} \cos(\xi/2) + i\hat{y} \sin(\xi/2)$. The detection axis is \hat{x} . At $\xi = 90^\circ$, which corresponds to circular polarization, the characteristic centrifugal suppression of low-energy ATI peaks¹² is clearly observed. However, this feature is not so prominent for $\xi = 80^\circ$, even though this represents an admixture of only about 1% of the opposite circular polarization in the laser intensity. Furthermore, at $\xi = 104^\circ$, where the admixture is also about 1% but the viewing direction is shifted by 90° , the suppression of low-energy peaks persists, suggesting sub-

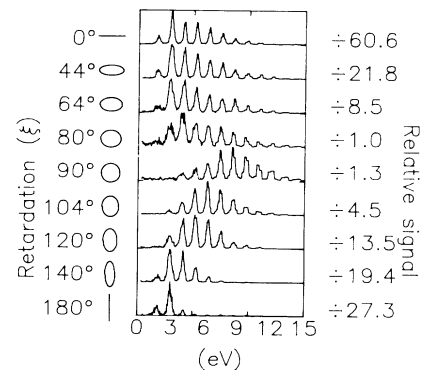


FIG. 1. Xenon photoelectron energy spectra as a function of the laser polarization for elliptically polarized light. The laser peak intensity is $5 \times 10^{13} \text{ W/cm}^2$.

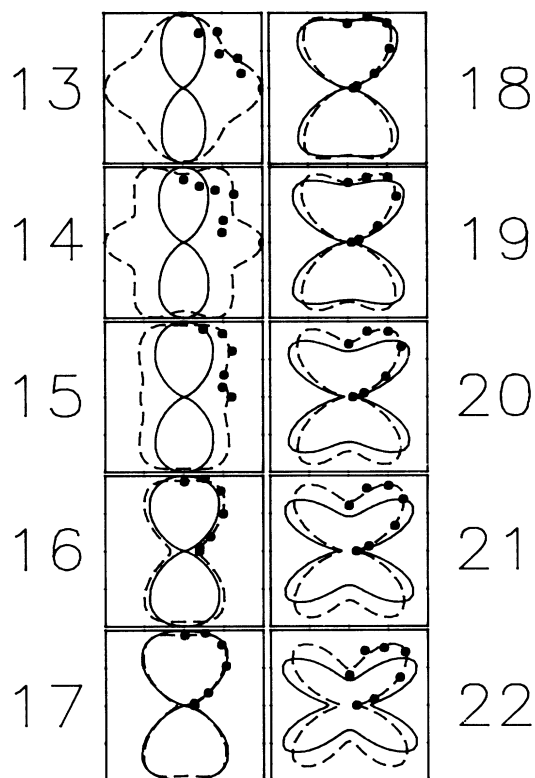


FIG. 2. Xe photoelectron angular distributions are plotted for different number of photons absorbed for 1064-nm elliptically polarized light at a retardation of $\xi=80^\circ$ and laser peak intensity of 5×10^{13} W/cm². At least eleven photons are required for ionization. The data points, represented by circles, were taken from 0° to 90° in intervals of 15° . Dashed lines represent the fit described in the text. Solid lines are the theoretical calculations with the retardation angle of 70° , and $U_p=1$ eV.

stantial azimuthal anisotropy. Indeed, examination of the azimuthal (ϕ) angular distributions at $\xi=80^\circ$ for each of the electron peaks (Fig. 2) reveals the presence of distinct maxima and minima, which evolve as the number of absorbed photons increases. The nodes are particularly prominent for higher-energy electrons since final-state ponderomotive scattering washes out details of the angular distributions for slower electrons.⁹

Similar studies were performed in krypton at a peak laser intensity of approximately 2.4×10^{14} W/cm² (Figs. 3 and 4). The angular distributions at $\xi=80^\circ$ show even more dramatic departures from azimuthal isotropy.

The dashed lines drawn through the data in Figs. 2 and 4 are fits of the real coefficients a_k in the series

$$P(\phi) = \sum_{k=0}^n a_k \cos(2k\phi). \quad (1)$$

A series of this form is suggested by perturbation theory for n photon absorption with nearly circularly polarized light. In this case, the most probable final state has a

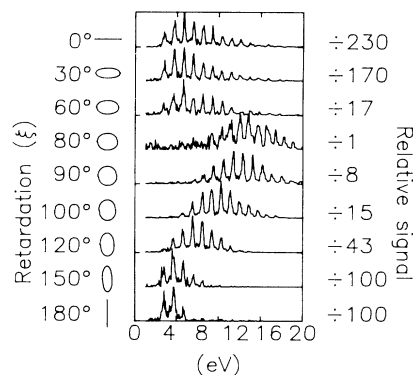


FIG. 3. Krypton photoelectron energy spectra as a function of the laser polarization, for elliptically polarized light. The laser peak intensity is 2.4×10^{14} W/cm².

magnetic quantum number change of $|\Delta m|=n$, the next most probable has $|\Delta m|=n-2$, and so on. Since the angular momentum eigenstates have an azimuthal angle (ϕ) dependence of $e^{im\phi}$, any linear superposition of final m states from a single initial state leads to a series of the form in Eq. (1). Furthermore, the symmetry of the angular distributions constrains all a_k to be real. The data were fitted by the first four terms. The numerical coefficients a_k for different order ATI peaks are shown in Tables I and II for xenon and krypton, respectively. This simple argument does not explain the relative magnitudes and signs of a_k and says nothing about the near cancellations among various terms that are required in order to reproduce the sharp nodes in the data.

A more elegant explanation of the data is obtained by theories in which the light is treated as a classical time-varying potential. Although these have been considered by a number of researchers,¹⁻⁷ to our knowledge no one has yet studied the problem in the general case of elliptically polarized light. We have found, however, that the extension from circular or linear polarization to arbitrary polarization is straightforward. As an example, we have adapted the approach used by Reiss and by Faisal,¹ who calculate the evolution of an atomic wave function under the influence of the Hamiltonian

$$H = -\frac{e\mathbf{p} \cdot \mathbf{A}(t)}{m_e c} + \frac{e^2 \mathbf{A}^2(t)}{2m_e c^2},$$

where $\mathbf{A}(t)$ is the vector potential of the electromagnetic field in the dipole approximation. In first order this procedure ignores the effect of the Coulomb potential on the final wave function, and Reiss cautions that its validity is questionable for long-range potentials. Nonetheless, it displays many features seen in these experiments, such as the number and relative magnitude of ATI peaks, and the suppression of low-energy peaks for circular polarization.³ It is therefore a useful starting point for this analysis. We have generalized the theory for elliptically polarized light. The details of the calculation will be

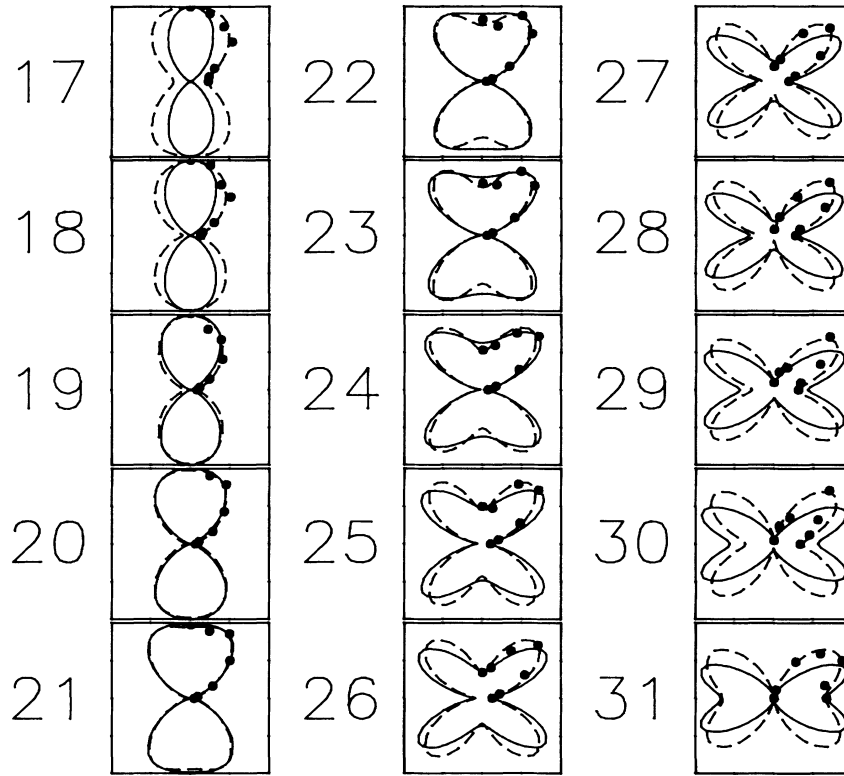


FIG. 4. Kr photoelectron angular distributions are plotted for a different number of photons absorbed for 1064-nm elliptically polarized light at a retardation of $\xi = 80^\circ$ and laser peak intensity of 2.4×10^{14} W/cm². At least twelve photons are required for ionization. The data points, represented by circles, were taken from 0° to 90° in intervals of 15° . Dashed lines represent the fit described in the text. Solid lines are the theoretical calculations with the retardation angle of 70° , and $U_p = 2$ eV.

presented elsewhere. The angular distribution for photoelectrons which have absorbed k photons is given by the following expression, where θ and ϕ are the polar and azimuthal photoemission angles, respectively:

$$\frac{dW}{d\Omega} = \Gamma_0(U_p, k) |\tilde{\Phi}(p_f, \Omega)|^2 \left| \sum_{m=-\infty}^{\infty} J_m(\alpha) J_{k+2m}(\beta) e^{i(k+2m)\chi} \right|^2. \quad (2)$$

Here J_m 's are cylindrical Bessel functions. Also $|\tilde{\Phi}|^2$ is the momentum distribution function of the initial state, evaluated at $p_f = [2m_e(kh\nu + E_G - U_p)]^{1/2}$, where E_G is the atomic ground-state energy and $U_p = e^2 |\mathbf{A}|^2 / 2m_e c^2$ is the ponderomotive potential. In addition,

$$\alpha = U_p \cos(\xi) / 2h\nu,$$

$$\beta = \frac{2}{h\nu} \sin(\theta) [U_p(kh\nu + E_G - U_p)(1 + \cos\xi \cos 2\phi)]^{1/2},$$

and

$$\chi = \arctan[\tan(\phi)\tan(\xi/2)].$$

The prefactor Γ_0 in Reiss's model is

$$\Gamma_0 = \frac{[2m^3 h^3 v^5 (k + E_G/h\nu - U_p/h\nu)]^{1/2}}{2\pi} \left(k - \frac{U_p}{h\nu} \right)^2,$$

which contains only angle-independent factors.

A complete comparison between theory and experi-

TABLE I. Fitting coefficients for xenon ATI angular distributions in Fig. 2.

| Photons absorbed | a_0 | a_1 | a_2 | a_3 |
|------------------|-------|--------|--------|-------|
| 13 | 0.818 | -0.014 | 0.114 | 0.021 |
| 14 | 0.765 | -0.073 | 0.028 | 0.116 |
| 15 | 0.781 | -0.257 | -0.025 | 0.062 |
| 16 | 0.625 | -0.439 | -0.066 | 0.062 |
| 17 | 0.610 | -0.483 | -0.093 | 0.066 |
| 18 | 0.616 | -0.479 | -0.145 | 0.075 |
| 19 | 0.623 | -0.438 | -0.213 | 0.065 |
| 20 | 0.656 | -0.384 | -0.266 | 0.049 |
| 21 | 0.680 | -0.307 | -0.308 | 0.032 |
| 22 | 0.648 | -0.190 | -0.358 | 0.005 |

TABLE II. Fitting coefficients for krypton ATI angular distributions in Fig. 4.

| Photons absorbed | a_0 | a_1 | a_2 | a_3 |
|------------------|-------|--------|--------|-------|
| 17 | 0.626 | -0.413 | -0.039 | 0.033 |
| 18 | 0.591 | -0.449 | -0.045 | 0.002 |
| 19 | 0.526 | -0.448 | -0.011 | 0.002 |
| 20 | 0.572 | -0.498 | -0.044 | 0.031 |
| 21 | 0.594 | -0.509 | -0.107 | 0.059 |
| 22 | 0.612 | -0.424 | -0.224 | 0.067 |
| 23 | 0.604 | -0.361 | -0.276 | 0.060 |
| 24 | 0.588 | -0.258 | -0.325 | 0.035 |
| 25 | 0.586 | -0.217 | -0.344 | 0.047 |
| 26 | 0.543 | -0.110 | -0.357 | 0.001 |
| 27 | 0.540 | -0.019 | -0.395 | 0.018 |
| 28 | 0.524 | 0.087 | -0.389 | 0.011 |
| 29 | 0.476 | 0.135 | -0.320 | 0.063 |
| 30 | 0.493 | 0.157 | -0.320 | 0.027 |
| 31 | 0.590 | 0.350 | -0.287 | 0.031 |

ment *must* take into account the spatial and temporal distribution of the laser pulse, ponderomotive scattering, and depletion of the interaction region. However, even without these added complications, the results of the calculation of Eq. (2) applied to the xenon and krypton data bear remarkable similarity to the experiment (Figs. 2 and 4). There are, however, important discrepancies that point to deficiencies in the theory: (1) The retardation angle used in the calculations was $\xi=70^\circ$ while the data were obtained for $\xi=80^\circ$. (2) The rate predicted by the theory at a given intensity is far below the observed rate. Although these discrepancies are serious, the strong qualitative agreement between theoretical and experimental angular distributions gives some encouragement for these theories.

In conclusion, we have found that ATI spectra and angular distributions are strongly dependent on the retardation of the laser polarization, particularly if the polarization is nearly circular. Results of elliptical polarization ATI experiments can be useful tests of perturbative and nonperturbative theories of atomic photoionization in intense fields.

We wish to acknowledge useful conversations with R. Freeman, T. McIlrath, and H. Reiss, and technical advice and assistance by J. Custer.

^(a)Also at Physics Department, Columbia University, New York, NY 10027.

¹H. R. Reiss, Phys. Rev. A **22**, 1786 (1980). In lowest order (used here), this theory ignores the effect of the Coulomb potential on the evolving wave function. This approximation was derived previously by F. H. M. Faisal, J. Phys. B **6**, L89 (1973).

²L. V. Keldysh, Zh. Eksp. Theor. Fiz. **47**, 1945 (1964) [Sov. Phys. JETP **20**, 1307 (1965)].

³H. R. Reiss, J. Phys. B **20**, L79 (1987).

⁴R. Shakeshaft, J. Opt. Soc. Am. B **4**, 705 (1987); W. Becker, R. R. Schlicher, M. O. Scully, and K. Wodkiewicz, J. Opt. Soc. Am. B **4**, 743 (1987); J. Kupersztynch, Europhys. Lett. (to be published); Shih-I Chu and R. Y. Yin, J. Opt. Soc. Am. B **4**, 720 (1987).

⁵H. G. Muller, A. Tip, and M. J. van der Wiel, J. Phys. B **16**, L679 (1983); H. G. Muller, and A. Tip, Phys. Rev. A **30**, 3039 (1984); R. Blumel and R. Meir, J. Phys. B **18**, 2835 (1985); M. Gavrilu and J. Z. Kaminski, Phys. Rev. Lett. **52**, 613 (1984); C. Cohen-Tannoudji, J. Dupont-Roc, C. Fabre, and G. Grynberg, Phys. Rev. A **8**, 2747 (1973); M. Crance and M. Aymar, J. Phys. B **13**, L421 (1980); Shih-I Chu and J. Cooper, Phys. Rev. A **32**, 2769 (1985); A. Szoke, J. Phys. B **18**, L427 (1985); M. Lewenstein, J. Mostowski, and M. Trippenbach, J. Phys. B **18**, L461 (1985); A. Szoke, Lawrence Livermore National Laboratory Report No. 93156, 1986 (to be published).

⁶Z. Bialynicka-Birula, J. Phys. B **17**, 3091 (1984); M. Edwards, L. Pan, and L. Armstrong, Jr., Phys. B **17**, L515 (1984); Z. Deng and J. H. Eberly, Phys. Rev. Lett. **53**, 1810 (1984), and J. Opt. Soc. Am. B **2**, 486 (1985); K. Rzazewski and R. Grobe, Phys. Rev. A **33**, 1855 (1986); J. Javanainen and J. H. Eberly, to be published.

⁷M. Mittleman, *Introduction to the Theory of Laser Atom Interactions* (Plenum, New York, 1982).

⁸Y. Gontier and M. Trahin, J. Phys. B **13**, 4383 (1980).

⁹R. R. Freeman, T. J. McIlrath, P. H. Bucksbaum, and M. Bashkansky, Phys. Rev. Lett. **57**, 3156 (1986).

¹⁰H. J. Humpert, H. Schwier, R. Hippler, and H. O. Lutz, Phys. Rev. A **32**, 3787 (1985); D. Feldman *et al.*, J. Phys. B **19**, L141 (1986); M. Bashkansky, P. H. Bucksbaum, R. R. Freeman, T. J. McIlrath, L. F. DiMauro, and J. Custer, in *Short Wavelength Coherent Radiation: Generation and Applications*, edited by D. T. Attwood and J. Bokor (American Institute of Physics, New York, 1986), p. 174.

¹¹T. J. McIlrath, P. H. Bucksbaum, R. R. Freeman, and M. Bashkansky, Phys. Rev. A **35**, 4611 (1987).

¹²P. H. Bucksbaum, M. Bashkansky, R. R. Freeman, T. J. McIlrath, and L. F. DiMauro, Phys. Rev. Lett. **56**, 2590 (1986).